JACS
JOURNAL OF THE AMERICAN CHEMICAL SOCIETY
Article
pubs.acs.org/JACS

Efficient Removal and Recovery of Uranium by a Layered Organic–Inorganic Hybrid Thiostannate

Mei-Ling Feng,[†,‡] Debajit Sarma,[‡] Xing-Hui Qi,[†] Ke-Zhao Du,[†] Xiao-Ying Huang,[†] and Mercouri G. Kanatzidis*[,‡]

[†]State Key Laboratory of Structural Chemistry, Fujian Institute of Research on the Structure of Matter, Chinese Academy of Sciences, Fuzhou, Fujian 350002, P. R. China

[‡]Department of Chemistry, Northwestern University, 2145 Sheridan Road, Evanston, Illinois 60208, United States

Supporting Information

ABSTRACT: Uranium is important in the nuclear fuel cycle both as an energy source and as radioactive waste. It is of vital importance to recover uranium from nuclear waste solutions for further treatment and disposal. Herein we present the first chalcogenide example, $(Me_2NH_2)_{1.33}(Me_3NH)_{0.67}Sn_3S_7 \cdot 1.25H_2O$ (FJSM-SnS), in which organic amine cations can be used for selective UO_2^{2+} ion-exchange. The UO_2^{2+}-exchange kinetics perfectly conforms to pseudo-second-order reaction, which is observed for the first time in a chalcogenide ion-exchanger. This reveals the chemical adsorption process and its ion-exchange mechanism. FJSM-SnS has excellent pH stability in both strongly acidic and basic environments (pH = 2.1−11), with a maximum uranium-exchange capacity of 338.43 mg/g. It can efficiently capture UO_2^{2+} ions in the presence of high concentrations of Na^+, Ca^{2+}, or HCO_3^- (the highest distribution coefficient K_d value reached 4.28×10^4 mL/g). The material is also very effective in removing of trace levels of U in the presence of excess Na^+ (the relative amounts of U removed are close to 100%). The $UO_2^{2+} \cdots S^{2-}$ interactions are the basis for the high selectivity. Importantly, the uranyl ion in the exchanged products could be easily eluted with an environmentally friendly method, by treating the UO_2^{2+}-laden materials with a concentrated KCl solution. These advantages coupled with the very high loading capacity, low cost, environmentally friendly nature, and facile synthesis make FJSM-SnS a new promising remediation material for removal of radioactive U from nuclear waste solutions.

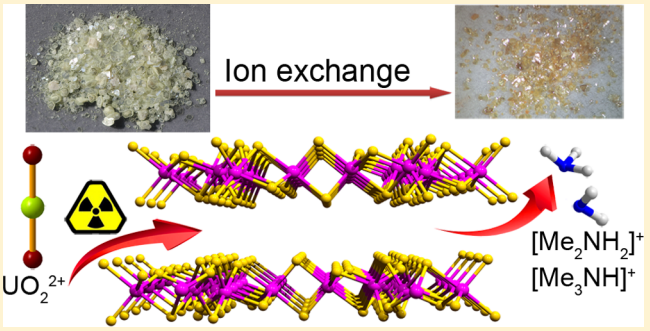

INTRODUCTION

Currently, nuclear power provides robust low-cost electrical power with no greenhouse gas emissions. Nuclear energy and the nuclear fuel cycle mandate strict management and safeguards that require the removal and recovery of hazardous radionuclides from nuclear waste. Uranium is one of the radioactive elements in nuclear wastes,[1] occurring in the form of soluble UO_2^{2+}.[2] U(VI) and U(IV) are the two most common species in the natural environment. U(VI) dissolves in water as the uranyl cation UO_2^{2+}, and it has significant mobility, which can cause it to easily enter into the food chain with serious health effects.[3,4] In addition, the oceans are a potential huge resource, containing over 4 billion tons of uranium (at about 3.3 ppb), which could supply uranium for nuclear energy for several thousand years.[5−7] Thus, it is strategically and ecologically important to capture U(VI) from aqueous solutions for further treatment and disposal.

Many methods have been investigated to remove uranium from nuclear waste, such as co-precipitation,[8,9] solvent extraction,[10,11] membrane filtration,[12] adsorption,[13,14] and adsorption/ion-exchange.[15−17] Adsorption and adsorption/ion-exchange are most attractive because of their low cost, ease of operation, and high efficiency.[18,19] Many adsorbents or ion-exchangers have been reported, such as clays,[20] zeolites,[21] titanate,[17,22] birnessite,[15] modified activated carbon,[23] gallocyanine-grafted hydro-gel,[24] nanoporous polymers,[25] magnetic ion-imprinted composite,[26] metal−organic frameworks,[27−29] and so on. The organics among them show stability problems, and the conventional inorganic materials tend to be efficient only in a narrow range of pH and often have low selectivity.[30] In recent years, the metal chalcogenides have emerged as a new class of inorganic ion-exchangers exhibiting high ion-exchange capacity and good selectivity for metal ions such as Cs^+, Sr^{2+}, Hg^{2+}, Pb^{2+}, and Cd^{2+}.[31−38] Compared to oxides, chalcogenides have advantages such as more flexible frameworks. They can also exhibit strong affinity for soft Lewis acidic metal ions because of the soft Lewis basic chalcogen atoms. This soft−soft interaction acts as a driving force in the process of ion-exchange and can lead to high selectivity for certain metal ions.[32,33,36] Although UO_2^{2+} is widely regarded as a hard Lewis acid cation, our previous results suggested that sulfides can be effective for

Received: July 16, 2016
Published: September 1, 2016

DOI: 10.1021/jacs.6b07351
J. Am. Chem. Soc. 2016, 138, 12578−12585

UO_2^{2+} capture by strong $UO_2^{2+}\cdots S^{2-}$ bonding interactions.[39] These results showed that the UO_2^{2+} ion is a softer Lewis acid center than previously thought. So far, only a few chalcogenide materials for UO_2^{2+} capture have been described, including $K_{2x}Mn_xSn_{3-x}S_6$ (KMS-1),[39] $K_{2x}Sn_{4-x}S_{8-x}$ (x = 0.65−1, KTS-3),[40] polysulfide/layered double hydroxide composites (S_x-LDH, x = 2, 4),[41] and chalcogels.[42]

The organic amine cations allow for wide tunability and flexibility.[35,36,43−46] Several new chalcogenide ion-exchange materials have been reported with organic ammonium ions as counterions and structure-directing agents, such as $[DPAH]_5In_5Sb_6S_{19}\cdot 1.45H_2O$ (DPA = dipropylamine),[43] $[(Me)_2NH_2]_2Ga_2Sb_2S_7\cdot H_2O$,[36] $[(Me)_2NH_2]_2[GeSb_2S_6]$,[35] $[(Me)_2NH_2]_{0.75}[Ag_{1.25}SnSe_3]$,[47] and $[CH_3NH_3]_4[In_4SbS_9SH]$.[48] These examples confirm that the protonated organic amine cations (typically $[Me_2NH_2]^+$, $[CH_3NH_3]^+$, and $DPAH^+$) in chalcogenides can be ion-exchanged with Cs^+ and Sr^{2+} ions, etc. However, organic amine cations in chalcogenides have not been documented, to date, for selective UO_2^{2+} ion-exchange.

Herein, we report the ion-exchange properties of a layered microporous sulfide, $(Me_2NH_2)_{1.33}(Me_3NH)_{0.67}Sn_3S_7\cdot 1.25H_2O$ (FJSM-SnS), toward UO_2^{2+}. Previously this material was shown to be a very efficient ion-exchanger for Cs^+ and Sr^{2+} ions.[46] FJSM-SnS can be prepared on a large scale by a straightforward one-step low-cost solvothermal route.[46] Its maximum uranium-exchange capacity (q_m) is 338.43 mg/g, comparable to those of the best reported uranium adsorbents[39−41] and much higher than those of commercial UO_2^{2+} scavengers.[49−51] Specifically, the material is capable of selective removal of uranyl ions even when a high concentration of Na^+, Ca^{2+}, or HCO_3^- is present and can keep its robust framework over a wide pH range of 2.1−11. Also, its kinetics perfectly conforms to pseudo-second-order reaction, which is observed in the ion-exchange process of a chalcogenide ion-exchanger for the first time. The pseudo-second-order kinetic model fitting indicates that the rate-limiting step in the adsorption process is chemical adsorption, further confirming the mechanism of ion-exchange. Moreover, the uranyl in corresponding exchanged products could be easily eluted by treating the UO_2^{2+}-laden materials with a concentrated KCl solution. Therefore, these advantages coupled with the very high loading capacity, low cost, environmentally friendly nature, and facile syntheses make FJSM-SnS promising for the removal and recovery of uranyl ions from very complex aqueous solutions.

EXPERIMENTAL SECTION

Materials and Synthesis. FJSM-SnS was synthesized using $SnCl_4\cdot 5H_2O$ (98%, Sigma-Aldrich), elemental sulfur (5N Plus Inc.), dimethylamine solution (40% in water, Sigma-Aldrich), and water by the solvothermal method at 180 °C as we previously reported.[46] The *in situ* generation of $[Me_3NH]^+$ from the solvent Me_2NH was discussed and confirmed in our previous report.[46]

UO_2^{2+} Ion-Exchange Experiments. A typical ion-exchange experiment of FJSM-SnS with $UO_2(NO_3)_2\cdot 6H_2O$ is as follows. To a solution of $UO_2(NO_3)_2\cdot 6H_2O$ (5.0 mg) in water (10 mL) was added the ground polycrystalline powder of FJSM-SnS (10.0 mg). The mixture was kept under magnetic stirring for 24 h at room temperature. The ion-exchanged material was then centrifuged and isolated by filtration (through filter paper, Whatman no. 1), washed several times with water and acetone, and dried in air. The concentrations of metal ions in the filtered solution were determined using inductively coupled plasma−atomic emission spectroscopy (ICP-OES) and, for extra low ion concentration (≤200 ppb), inductively coupled plasma−mass spectroscopy (ICP-MS).

The kinetic study of UO_2^{2+} ion-exchange by FJSM-SnS was carried out as follows. Ion-exchange experiments were performed for various reaction times (3, 6, 15, 30, 60, 120, 240, and 1200 min). A 10 mg sample of FJSM-SnS powder was weighed into 10 mL of water solution containing 1 ppm of uranium, and the mixtures were kept under magnetic stirring. The suspensions were filtered at the various reaction time, and the filtrates were analyzed by ICP-MS (Table S1).

Experiments studying the pH dependence of UO_2^{2+} ion-exchange were also carried out (Table S2). Solutions of UO_2^{2+} with different pH (in the range of 2−11) were prepared. The pH values were achieved by diluting the commercial standards (1000 ppm) with HCl or NaOH solution. The initial concentrations of uranium were 0.17−3.58 ppm. The experiments on the pH dependence of UO_2^{2+} ion-exchange were done by batch method at a V/m ratio of 1000 mL/g (V of 10 mL, m of 10 mg), room temperature, and 24 h contact time. All samples were isolated by filtration and analyzed.

It is well known that the aqueous solution of $UO_2(NO_3)_2\cdot 6H_2O$ is acidic. The higher the concentration of aqueous solution of $UO_2(NO_3)_2\cdot 6H_2O$ the stronger the acidity. Besides, the aqueous solution of uranium can hydrolyze at high pH. At the same time, the higher concentration of uranium, the lower the pH value of hydrolysis. So the pH values of the initial solutions with various concentrations of uranium (10−603 ppm) were adjusted using NaOH solution to the range of 4−7 in order to avoid hydrolysis and the super acidic condition. The isotherm experiments (Table S3) were done by batch method at V/m ratio of 1000 mL/g, room temperature, and 24 h contact time. All the samples were then took out and analyzed.

The ion-exchange experiments of UO_2^{2+} (U = 1 ppb−4 ppm) in the presence of excess NaCl, $NaNO_3$, $NaHCO_3$ (Na/U molar ratios = 6.36×10^3−3.45×10^7) (Tables S4 and S6), or $CaCl_2$ (Ca/U molar ratios = 2.89×10^2−6.05×10^4) (Table S5) were carried out using a V/m ratio of 1000 or 100 mL/g, and 24 h contact time. The simulated contaminated seawater and potable water samples were prepared by adding appropriate microliter amounts of U solutions to natural seawater and potable water, and a total of 100 mg of FJSM-SnS powder was weighed into a 10 mL sample of contaminated seawater or potable water. Natural seawater was from the Pacific Ocean near Sequim, Washington. Potable water was found in Evanston, Illinois. Then the typical ion-exchange experiments were performed (Table S6).

In order to elute the materials, UO_2^{2+}-laden samples of ∼5 mg were treated with 10 mL solutions containing 0.27 M concentrated KCl solution under magnetic stirring for 24 h at room temperature. UO_2^{2+}-laden samples were those obtained from the ion-exchange capacity experiments done for the isotherm study containing 603 ppm U. After this treatment, the filtered solution was analyzed for its U content with ICP-MS. The solid samples were analyzed by energy-dispersive spectroscopy (EDS) and powder X-ray diffraction (PXRD).

Characterization Techniques. The UV−vis/near-IR diffuse reflectance spectra of the ground samples were collected using a Shimadzu UV03010 PC double-beam, double-monochromator spectrophotometer in the wavelength range of 200−2500 nm. $BaSO_4$ powder was used as a reference and base material on which the powder sample was coated. Using the Kubelka−Munk equation the reflectance data were converted to absorption data as described earleir.[52,53]

The PXRD patterns were collected at room temperature with a CPS 120 INEL X-ray powder diffractometer with graphite monochromated Cu Kα radiation operating at 40 kV and 20 mA. EDS was performed with a Hitachi S-3400N-II scanning electron microscope (SEM) equipped with an ESED II detector. An accelerating voltage of 20 kV and 60 s acquisition time were used for elemental analysis.

X-ray photoelectron spectroscopy (XPS) of the FJSM-SnS and exchanged products were performed on ground powders using a Thermo Scientific ESCALAB 250 Xi spectrometer equipped with a monochromatic Al Kα X-ray source (1486.6 eV) operating at 300 W. Samples were analyzed under vacuum ($P < 10^{-8}$ mbar) with a pass energy of 150 eV (survey scans) or 25 eV (high-resolution scans). A low-energy electron flood gun was employed for charge neutralization. Ion beam etching was performed to clean off some of the surface

DOI: 10.1021/jacs.6b07351
J. Am. Chem. Soc. 2016, 138, 12578−12585

contamination. Prior to the XPS measurements, the crystalline powders were pressed on copper foil, mounted on stubs, and successively put into the entry-load chamber to pump. All peaks were referenced to the signature C 1s peak binding energy at 284.6 eV for adventitious carbon. The experimental peaks were fitted with Avantage software.

The concentrations of metal ions in the solution before and after UO_2^{2+} ion-exchange were analyzed using ThermoFisher iCap7600 ICP-OES and ThermoFisher iCapQ ICP-MS instrumentation. The ion-exchange samples were diluted to lower the concentrations below 200 ppb for ICP-MS.

RESULTS AND DISCUSSION

UO_2^{2+} Ion-Exchange of FJSM-SnS. The structure of FJSM-SnS features a 2D $[Sn_3S_7]_n^{2n-}$ anionic layer with large windows formed by 24-membered $[Sn_{12}S_{12}]$ rings from six $[Sn_3S_4]$ cores (Figure 1a). The $[Me_2NH_2]^+$, $[Me_3NH]^+$ cations,

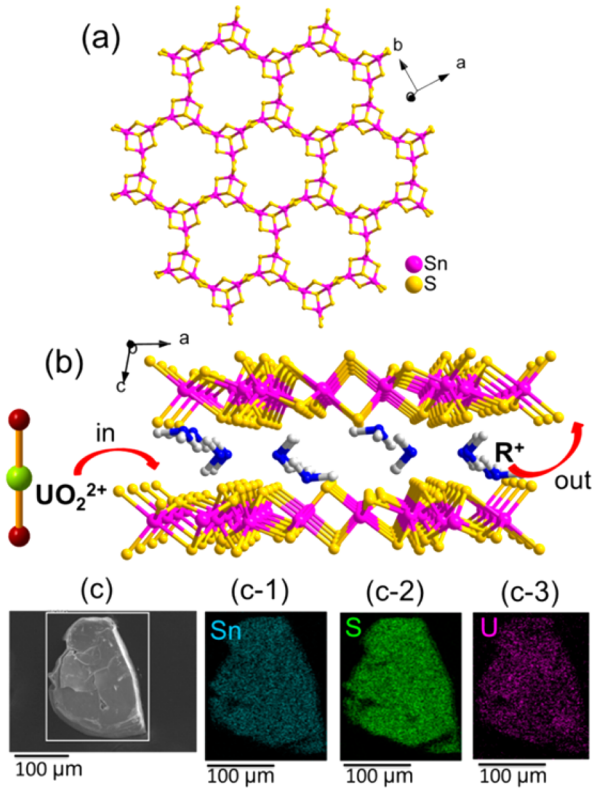

Figure 1. (a) View of the 2D $[Sn_3S_7]_n^{2n-}$ anionic layer with large windows parallel to the ab plane. (b) Intercalative mechanism of capture of UO_2^{2+} ions by FJSM-SnS through exchange of $[Me_2NH_2]^+$ and $[Me_3NH]^+$ cations (R^+ = $[Me_2NH_2]^+$, $[Me_3NH]^+$ cations). (c) SEM images of UO_2^{2+}-exchanged product and its elemental distribution maps of Sn (c-1), S (c-2), and U (c-3).

and water molecules occupy the interlayer space.[46] The $[Sn_3S_7]_n^{2n-}$ anionic layer exhibits a flexible framework that can distort somewhat in response to a variety of templating counter-cations, such as $[Me_4N]^+$,[54] Cs^+,[55] $[Me_3N]^+$,[56] $[DABCOH]^+$ (protonated 1,8-diazabicyclooctane),[57] QUIN (QUIN = quinuclidinium),[58] TBA (TBA = *tert*-butylamine),[58] $[NH_4]^+$, and $[Et_4N]^+$ ($[Et_4N]^+$ = tetraethylamine).[59] The structural characteristic of FJSM-SnS provides the prerequisite for UO_2^{2+} ion-exchange (Figure 1b). FJSM-SnS maintained the crystal shape after UO_2^{2+}-exchange, and its layered nature was more distinct after UO_2^{2+} ions intercalated in the layers. SEM images of pristine crystals and UO_2^{2+}-exchanged products are shown in Figure S1. The exchange of organic amine cations of FJSM-SnS by UO_2^{2+} was confirmed by ICP-OES, ICP-MS, EDS, and XPS. The EDS analyses of the products after ion-exchange showed that UO_2^{2+} entered the materials (Figure S2). Elemental mapping of the exchanged products confirmed the presence of captured uranium and its homogeneous distribution in the sample (Figure 1c).

The PXRD patterns of the UO_2^{2+}-exchanged products showed retention of the parent structure (Figure 2a). The

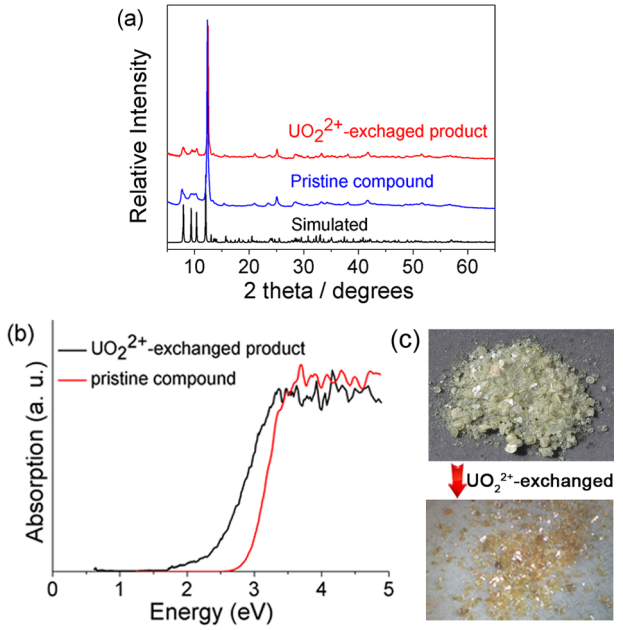

Figure 2. (a) PXRD patterns of pristine FJSM-SnS and UO_2^{2+}-exchanged products with the simulated pattern of FJSM-SnS. (b) Optical absorption spectra of FJSM-SnS and UO_2^{2+}-exchanged products. (c) Photos of FJSM-SnS and the darker colored UO_2^{2+}-exchanged products. In a solution (pH = 3.2) of $UO_2(NO_3)_2{\cdot}6H_2O$ (58.2 mg) in water (10 mL), the crystals of FJSM-SnS (21.3 mg) were added. Then the UO_2^{2+}-exchanged products were obtained.

optical absorption edge of FJSM-SnS is ~2.92 eV, and it red-shifts to ~2.49 eV for the UO_2^{2+}-exchanged products (Figure 2b). So the optical absorption edge of the UO_2^{2+}-exchanged products exhibits a significant red shift compared to the pristine compound. The lower optical absorption edge is consistent with the darker colors of the UO_2^{2+}-exchanged products (Figure 2c) and strongly suggests the presence of $UO_2^{2+}\cdots S^{2-}$ interactions. These bonding interactions of the inserted UO_2^{2+} ions and the S atoms of the framework reflect the significant soft Lewis acid character of the UO_2^{2+} ion.[39] Similar phenomena have been observed in other UO_2^{2+} ion-exchange materials such as KMS-1[39] and KTS-3.[40]

XPS of the pristine compound exhibit characteristic peaks for Sn 3d and S 2p, whereas two evident peaks at 382.0 and 392.9 eV, corresponding to U $4f_{7/2}$ and U $4f_{5/2}$ of U^{6+} centers, were observed in XPS spectra of the UO_2^{2+}-exchanged products, along with the Sn 3d and S 2p characteristic peaks (Figure 3). Moreover, it is worth noting that the peak observed for nitrogen in the XPS spectra of the exchanged products has been greatly weakened, indicating that the organic amines were exchanged by uranium (Figure 3d). Thus, the XPS analysis further demonstrates the successful uranyl ion-exchange, in good agreement with the EDS results.

DOI: 10.1021/jacs.6b07351
J. Am. Chem. Soc. 2016, 138, 12578−12585

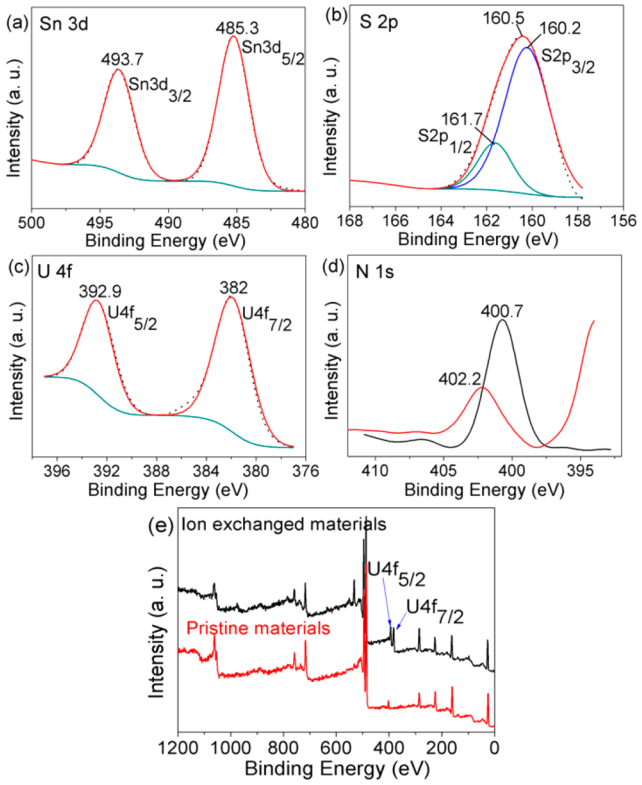

Figure 3. X-ray photoelectron spectra of tin (a), sulfur (b) for FJSM-SnS. (c) X-ray photoelectron spectrum of uranium for the ion-exchanged products. Black dotted and red solid lines represent experimental and overall fitting peaks, respectively. The green lines represent the fitting of background. One green convex line and one blue line are deconvoluted peaks for S $2p_{1/2}$ and S $2p_{3/2}$ in (b), respectively. Respective comparisons of experimental nitrogen spectra (d) and survey spectra (e) before (red line) and after ion-exchange (black line) are shown.

Kinetic Studies of UO_2^{2+} Ion-Exchange. The kinetics of UO_2^{2+} ion-exchange was investigated and showed that the concentrations of uranium (~1 ppm at V/m ratio of 1000 mL/g) decreased rapidly: the relative amount of U removed reached 80.3% after 1 h and increased to 91% after 20 h (Figure 4, Table S1). It is interesting that the kinetic data can be analyzed

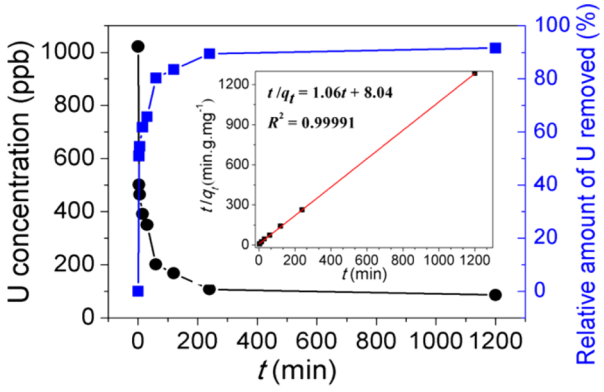

Figure 4. Kinetics of the UO_2^{2+} ion-exchange process with FJSM-SnS plotted as the U concentration (ppb) (black line) and the relative amount of U removed (%) (blue line) vs the time t (min), respectively. Inset: the plot of t/q_t vs t of the current kinetics data which is well fitted with the pseudo-second-order kinetic model.

according to the pseudo-second-order kinetics, which can be described by eq 1.

$$\frac{t}{q_t} = \frac{1}{k_2 q_e^{\,2}} + \frac{t}{q_e} \quad (1)$$

Here, k_2 is the pseudo-second-order rate constant of adsorption ($g \cdot mg^{-1} \cdot min^{-1}$). The quantities q_e and q_t are the amounts of metal ion adsorbed (mg/g) at equilibrium and at time t, respectively, and t is adsorption time (min). The plots of t/q_t vs t of the kinetics data showed perfect linear relation (the inset in Figure 4). So the data were found to be best fitted to the pseudo-second-order kinetic model with a correlation coefficient (R^2 = 0.99991) indicating that the rate-limiting step of the adsorption process is chemical adsorption,[60] in which q_e = 0.94 mg/g and k_2 = 0.14. This further confirms that the mechanism of adsorption is ion-exchange.[61] This model has been found to be appropriate for describing the kinetics of UO_2^{2+} sorption by other materials, such as amidoximated magnetite/graphene oxide composites,[60] ZnO nanorod arrays on cotton cloth,[61] and amidoxime-functionalized wool fibers.[62] However, this model has not been observed for UO_2^{2+} sorption by chalcogenides to date.

pH-Dependent UO_2^{2+} Ion-Exchange. The distribution coefficient K_d was measured over a broad pH range (2.1−11). K_d is a measurement of affinity and selectivity, described by eq 2. The ion-exchange efficiency, i.e., the relative amount of U removed (R), was calculated with eq 3.

$$K_d = \frac{V}{m}\frac{(C_0 - C_f)}{C_f} \quad (2)$$

$$R = \frac{(C_0 - C_f)}{C_0} \times 100\% \quad (3)$$

In eqs 2 and 3, C_0 and C_f represent the initial and equilibrium concentrations of the ions as measured by ICP.

Ion-exchange reactions of FJSM-SnS performed with UO_2^{2+} solutions (uranium concentration in the range of 0.17−3.58 ppm, V/m = 1000 mL/g) of various pH showed a very high percentage of uranium removal (>92%), and the high K_d values ranged from 1.32×10^4 to 2.64×10^4 mL/g in the pH range of 3.8−6.5 (Figure 5a, Table S2). Even in slightly alkali solution (the pH range of 7.3−8.4), the relative amounts of U removed and K_d values can still reach more than 69% and 2.29×10^3 mL/g, respectively (Table S2). In general, a material with a K_d value $>10^4$ mL/g is considered to be an excellent adsorbent.[31,63]

Clearly, FJSM-SnS is effective in removing uranium in slightly acidic, neutral, and slightly alkali conditions (pH range of 3.8−8.4). This is superior to some oxide ion-exchangers such as manganese oxides,[15] titanate,[17] and ZnO nanorod arrays on cotton cloth.[61] Generally, oxide ion-exchangers are active at pH > 4. FJSM-SnS contains S^{2-} ligands as soft basic sites, which display low affinity for hard proton ions, but high affinity for UO_2^{2+}. By contrast oxide materials are strongly interfered with proton cations which attach to the hard O^{2-} ions according to Lewis theory of acids and bases.[39]

In addition, the PXRD patterns of the ion-exchanged products (from the pH range 3.8−11) were similar to those of the pristine FJSM-SnS (Figure 5b). When the pH of the initial solution was adjusted to 2.1, a number of competitive proton cations also entered the interlayer space of FJSM-SnS. So the PXRD for exchanged product at pH = 2.1 showed a shift

DOI: 10.1021/jacs.6b07351
J. Am. Chem. Soc. 2016, 138, 12578−12585

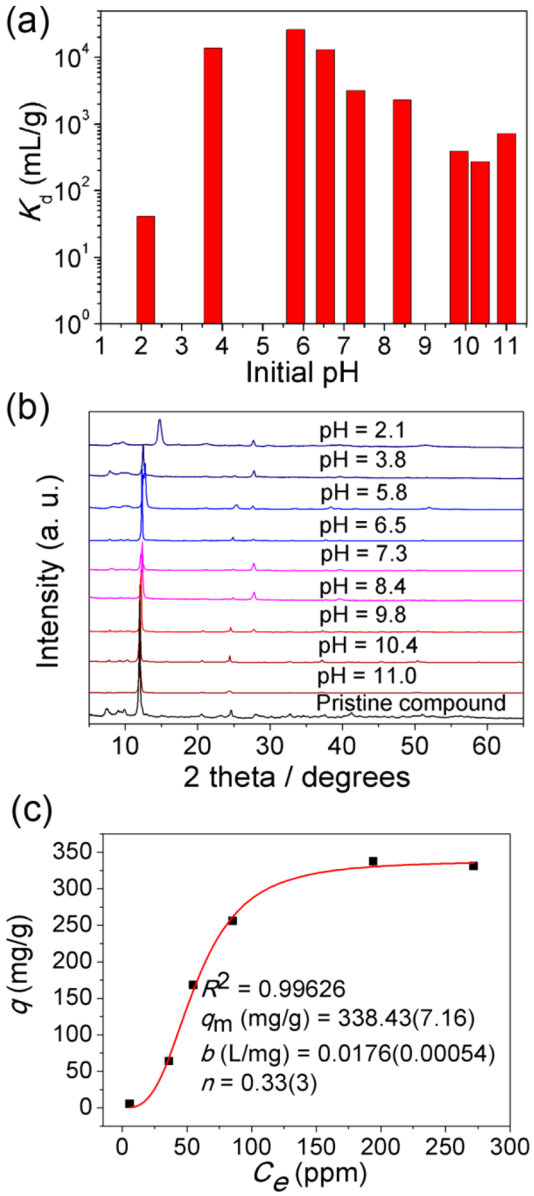

Figure 5. (a) Distribution coefficient K_d values of U at various initial pH values (C_0 in the range of 0.17−3.58 ppm for U, V/m = 1000 mL/g, at room temperature). (b) PXRD patterns of pristine and ion-exchanged compounds at various pH values. (c) Equilibrium data for UO_2^{2+} ion-exchange (pH in the range of 4−7, V/m = 1000 mL/g, at room temperature, 24 h contact time, initial U concentrations from 10 to 603 ppm). The solid red line is the fit of the data with the Langmuir−Freundlich isotherm model.

of the basal Bragg peak to higher 2θ angles (lower d-spacing) (Figure 5b), indicating that the interlayer distance decreased due to the smaller proton cations entering. The structural stability of FJSM-SnS, which exhibits acid and alkali resistance compared to the other UO_2^{2+} ion-exchangers, is thus impressive.[17,41,61]

Adsorption Isotherm Study of UO_2^{2+} Ion-Exchange. According to the results of pH-dependent UO_2^{2+} ion-exchange experiments, FJSM-SnS can retain high K_d values and amounts of U removed in the pH range of 3.8−8.5 (Table S2). To evaluate the ability of FJSM-SnS to absorb UO_2^{2+}, the isotherm experiments with various concentrations of uranium (10−603 ppm) in the pH range of 4−7 were carried out at room temperature (Table S3). The UO_2^{2+} equilibrium curve is graphed in Figure 5c, which is derived from the uranium concentration at equilibrium plotted against the capacity of U-exchange. The Langmuir−Freundlich equilibrium isotherm model can fit very well with a correlation coefficient (R^2 = 0.99626). The Langmuir isotherm model describes adsorption on a homogeneous surface and presumes that a maximum uptake exists. In this model, all the adsorption sites are assumed to have the same sorption activation energy. The energy of adsorption is thus constant and independent of surface coverage. It is also assumed that there is no transmigration of adsorbate from one site to another.[40,64,65] The Langmuir−Freundlich isotherm can be described by eq 4:

$$q = q_m \frac{(bC_e)^{1/n}}{1 + (bC_e)^{1/n}} \quad (4)$$

where q (mg/g) is the amount of cation adsorbed at equilibrium concentration C_e (ppm), q_m is the maximum cation adsorption capacity (mg/g), b (L/mg) is a constant related to the free energy of the exchange, and n is a constant. The value of q can be calculated from eq 5.

$$q = \frac{(C_0 - C_e)V}{m} \quad (5)$$

From Figure 5c, the maximum uranium-exchange capacity (q_m) of FJSM-SnS is 338.43(7.16) mg/g, very close to its theoretical value (337.85 mg/g) (Equation S1), which is comparable to those of the best uranium adsorbents.[39−41] We note that the q_m of FJSM-SnS for U is considerably higher than commercial resin products such as commercial phosphinic acid resin, Tulsion CH-96 (70 mg/g),[49] strong base AMBERSEP 920U Cl Resin (50 mg/g),[50] and ARSEN-X^{np} Purolite Resin (47 mg/g).[51] The above results suggest that FJSM-SnS has very high UO_2^{2+} ion-exchange capacity.

Effects of Na^+ and Ca^{2+} Cations and HCO_3^- Anion on UO_2^{2+} Ion-Exchange. Since very high concentrations of sodium ions and about 145 ppm of HCO_3^- anions are present in seawater, the performances of FJSM-SnS for UO_2^{2+} ion-exchange in the presence of a large excess of Na^+ and HCO_3^- were tested. We find that the relative amount of U removed and K_d value are 97.7% and 4.28 × 10^4 mL/g, respectively, in a competitive exchange experiment containing 0.3 M NaCl and 34 ppb U (Figure 6a, Table S4). Despite the presence of a tremendous (>10^4-fold) excess of NaCl or $NaNO_3$, FJSM-SnS is still able to maintain an exceptional ability to absorb UO_2^{2+} (≥92% U removal capacity), and K_d values were higher than 10^4 mL/g (Figure 6a, Table S4). So it is evident that FJSM-SnS has a strong preference and very high selectivity for UO_2^{2+} ions against Na^+. Even in the presence of HCO_3^- anions, FJSM-SnS can still capture UO_2^{2+} ions. For instance, in the cases of excess of HCO_3^- (145 ppm) with 10 ppb U, the relative amount of U removed and K_d value are 70.8% and 2.43 × 10^3 mL/g, respectively (Figure 6a, Table S4).

In addition, Ca^{2+} ions may also exist in high concentrations in wastewater and can be strong competitors for the ion-exchange of toxic ions in many absorbents.[39,41] Therefore, the UO_2^{2+} ion-exchange ability of FJSM-SnS in the presence of excess $CaCl_2$ was also explored. The results show that FJSM-SnS can still retain high relative amounts of U removed (62−84%), and K_d values for UO_2^{2+}/Ca^{2+} selectivity coefficient were more than 10^3 mL/g, even with a tremendous excess of $CaCl_2$ ($CaCl_2$:U molar ratio reached 6.05 × 10^4) (Figure 6b, Table

DOI: 10.1021/jacs.6b07351
J. Am. Chem. Soc. 2016, 138, 12578−12585

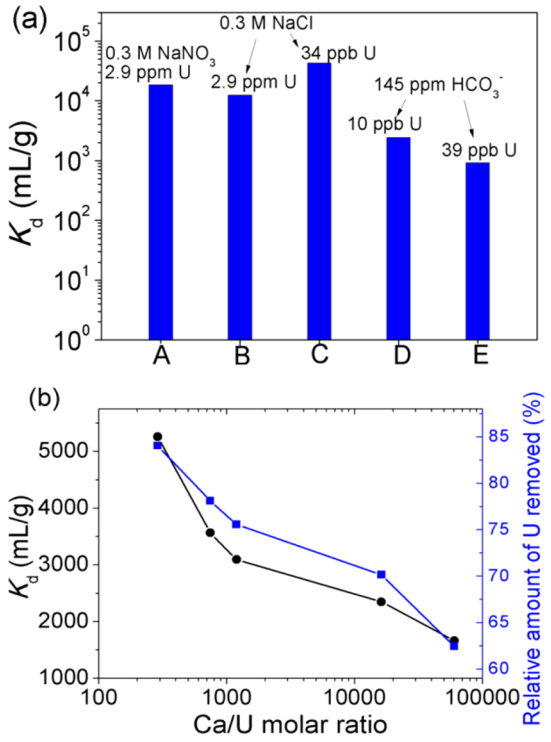

Figure 6. (a) Distribution coefficient K_d values (y axis) of U under different conditions (x axis) in a large excess of Na^+: A, 0.3 M $NaNO_3$ + 2.9 ppm U; B, 0.3 M NaCl + 2.9 ppm U; C, 0.3 M NaCl + 34 ppb U; D, 145 ppm of HCO_3^- + 10 ppb U; E, 145 ppm of HCO_3^- + 39 ppb U). (b) Variation of the distribution coefficient K_d values of U (black line) and the relative amounts of U removed (%) (blue line) with the Ca/U molar ratio. V/m = 1000 mL/g, at room temperature, 24 h contact time.

S5). These data indicate that FJSM-SnS has a high selectivity and strong affinity for UO_2^{2+} over a large excess of Ca^{2+}.

UO_2^{2+} Ion-Exchange toward Trace UO_2^{2+} Ions, Contaminated Seawater, and Contaminated Potable Water. Considering that large amounts of uranium exist in seawater, and that nuclear power accidents can cause contamination of seawater and potable water by uranium, we also examined the UO_2^{2+} ion-exchange performance of FJSM-SnS toward trace UO_2^{2+} ions, simulated contaminated seawater, and contaminated potable water (Table S6). In the exchange experiments containing 0.3 M NaCl or 0.15 M $NaNO_3$ and trace UO_2^{2+} ions (1.6–2.1 ppb), remarkably the removal efficiencies of FJSM-SnS for U are almost close to 100% (Table S6), higher than other chalcogenide scavengers for U in the same condition.[39,41] Even in the presence of 0.3 M NaCl and 145 ppm of HCO_3^- anions, FJSM-SnS still had the very high amount of U removed of 93.3% for UO_2^{2+} ions (Table S6). FJSM-SnS can also decrease the U concentration of the simulated contaminated seawater (Table S6). Compared with the complex contaminated seawater condition, FJSM-SnS can efficiently capture uranyl ions in simulated contaminated potable water and maintain decent relative amounts of U removed (59% and 68.6%, Table S6).

Elution. UO_2^{2+}-exchanged FJSM-SnS materials (UO_2-FJSM-SnS) were used in the elution experiments by applying excess KCl solution. The results indicate that uranyl in corresponding exchanged products can be easily eluted by treating with a concentrated KCl solution (0.27 M), which was confirmed by EDS, ICP-MS, and XRD. The EDS analyses of the eluted products showed that K^+ ions completely replaced the UO_2^{2+} ions with the near composition of $KSn_{1.73}S_{3.56}$ (Figure S3). The elemental distribution mapping showed the presence of K^+ ions with a homogeneous distribution in the sample (Figure 7). At the same time, 270 ppb of U in KCl

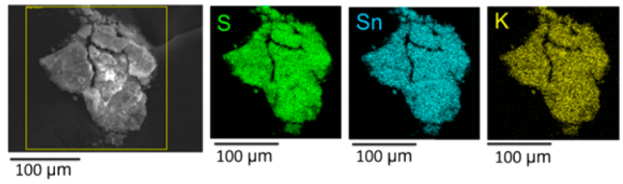

Figure 7. SEM image of the eluted products and elemental distribution maps of S, Sn, and K.

solution after the elution was detected using ICP-MS. The PXRD pattern of eluted products is showed in Figure S4. This high elution efficiency and easy separation from the treated medium highlight the great potential of the material for extraction of uranium from nuclear waste.

Organic Amine Cations and UO_2^{2+} Ion-Exchange. Thus far, organic amines have been extensively applied in the preparation of new chalcogenides.[66,67] One of the roles of organic cations as structure-directing agents is to fill the void space in the inorganic framework, balancing the negative charge. These cations interact with the framework with weak electrostatic interactions, hydrogen bonds, and van der Waals forces. In this case, the organic cations are mobile and exchangeable with other guest cations. For instance, protonated monoamines such as $[CH_3NH_3]^+$, $[Me_2NH_2]^+$, and $DPAH^+$ can be exchanged by Cs^+ and Sr^{2+} ions with the high ion-exchange capacity.[35,43,45,46] The current study, where the mixed $[Me_2NH_2]^+$ and $[Me_3NH]^+$ cations exchange with uranyl ions, opens a new direction for the preparation of new chalcogenide UO_2^{2+} ion-exchanger. In particular, FJSM-SnS has very high UO_2^{2+} ion-exchange capacity, with q_m = 338.43 mg/g, and exhibits high removal U efficiency and excellent selectivity for U, even in the presence of high levels of Na^+, Ca^{2+}, or HCO_3^-. A comparison of U removal efficiency between FJSM-SnS and various other adsorbents is shown in Table S7. The large ion-exchange capacity, high removal efficiency, and excellent selectivity for U are attributed to two favorable factors. One is the stronger affinity of soft Lewis basic S^{2-} ions from its framework for relatively soft Lewis acidic UO_2^{2+} ions to form $UO_2^{2+}\cdots S^{2-}$ interactions. These are stronger than the electrostatic interactions with the $[Me_2NH_2]^+$ and $[Me_3NH]^+$ cations, Na^+, or Ca^{2+} ions. Similar phenomena indicative of $UO_2^{2+}\cdots S^{2-}$ interactions have been observed in KMS-1[39] and KTS-3.[40] The other factor is its two-dimensional flexible framework which enables the guest cations to diffuse rapidly in and out of the structure. This point has also been demonstrated by its excellent Cs^+ and Sr^{2+} ion-exchange performances.[46] Here UO_2^{2+}-exchange results further strengthen our understanding for selective uranium separation in a variety of aqueous media.

CONCLUDING REMARKS

FJSM-SnS presents the first example of a chalcogenide in which organic amine cations can be used for selective UO_2^{2+} ion-exchange. This study demonstrates that the introduction of organic amine cations into chalcogenides is an efficient strategy to develop new, highly efficient, and inexpensive chalcogenide UO_2^{2+} scavengers. FJSM-SnS has high exchange capacity and

DOI: 10.1021/jacs.6b07351
J. Am. Chem. Soc. 2016, 138, 12578–12585

selectivity for UO_2^{2+} ions, with excellent acid and alkali resistance (pH = 2.1−11). These characteristics are due to the strong affinity of the soft Lewis basic S^{2-} ions for relatively softer Lewis acidic UO_2^{2+} ions as well as to the flexible layered framework. The maximum uranium-exchange capacity of FJSM-SnS, at 338.43 mg/g, is much higher than those of commercial UO_2^{2+} scavengers. For a chalcogenide, it is observed for the first time that the kinetics perfectly conforms to pseudo-second-order reaction in the ion-exchange process. This reveals the chemical adsorption process and its ion-exchange mechanism. In addition, FJSM-SnS can efficiently capture UO_2^{2+} ions in the presence of the high concentrations of Na^+, Ca^{2+}, or HCO_3^-. It is very effective for the removal of trace levels of U even against Na^+ (the relative amounts of U removed are close to 100%). Furthermore, uranyl in corresponding exchanged products can be easily eluted by a cost-affordable and environmentally friendly method. In summary, the advantages of FJSM-SnS include (i) low cost and facile synthesis, (ii) excellent acid and alkali resistance, (iii) high removal efficiency for uranyl ions, and (iv) easy, cheap, and efficient elution. These advantages render FJSM-SnS a promising material for remediation of radioactive U from nuclear waste solutions.

■ ASSOCIATED CONTENT

Supporting Information

The Supporting Information is available free of charge on the ACS Publications website at DOI: 10.1021/jacs.6b07351.

Tables S1−S7, showing data for the UO_2^{2+}-exchange of FJSM-SnS in kinetic, pH-dependent experiments, isotherm study, in the presence of a large excess of Na^+ ions, with competitive Ca^{2+} ions, toward trace UO_2^{2+} ions, contaminated seawater, and contaminated potable water, and U removal efficiency of various sorbents in this work; calculation of the theoretical ion-exchange capacity (Equation S1); and Figures S1−S4, showing SEM images of pristine FJSM-SnS crystals and UO_2^{2+}-exchanged product, EDS analysis of UO_2^{2+}-exchanged products and the eluted product, and PXRD patterns of eluted products, UO_2^{2+}-exchanged products, and the pristine compound (PDF)

■ AUTHOR INFORMATION

Corresponding Author

*m-kanatzidis@northwestern.edu

Notes

The authors declare no competing financial interest.

■ ACKNOWLEDGMENTS

We thank the National Science Foundation of the United States for support of this research (Grant DMR-1410169). We also thank the National Science Foundations of China (Nos. 21373223 and 21521061), the 973 programs (2014CB845603 and 2012CB821702), and Chunmiao project of Haixi Institute of Chinese Academy of Sciences (CMZX-2014-001).

■ REFERENCES

(1) Craft, E. S.; Abu-Qare, A. W.; Flaherty, M. M.; Garofolo, M. C.; Rincavage, H. L.; Abou-Donia, M. B. *J. Toxicol. Environ. Health, Part B* **2004**, *7*, 297−317.

(2) (a) Boice, J. D., Jr. *J. Radiol. Prot.* **2012**, *32*, N33−N40. (b) Norrström, A. C.; Löv, Å. *Appl. Geochem.* **2014**, *51*, 148−154.

(3) Abdelouas, A.; Lu, Y. M.; Lutze, W.; Nuttall, H. E. *J. Contam. Hydrol.* **1998**, *35*, 217−233.

(4) O'Loughlin, E. J.; Kelly, S. D.; Cook, R. E.; Csencsits, R.; Kemner, K. M. *Environ. Sci. Technol.* **2003**, *37*, 721−727.

(5) Davies, R. V.; Kennedy, J.; Mcilroy, R. W.; Spence, R.; Hill, K. M. *Nature* **1964**, *203*, 1110−1115.

(6) Kim, J.; Tsouris, C.; Mayes, R. T.; Oyola, Y.; Saito, T.; Janke, C. J.; Dai, S.; Schneider, E.; Sachde, D. *Sep. Sci. Technol.* **2013**, *48*, 367−387.

(7) Lu, Y. *Nat. Chem.* **2014**, *6*, 175−177.

(8) Zou, W. H.; Song, J. Y.; Li, K.; Han, R. P. *Adsorpt. Sci. Technol.* **2010**, *28*, 313−325.

(9) Baeza, A.; Fernandez, M.; Herranz, M.; Legarda, F.; Miro, C.; Salas, A. *Water, Air, Soil Pollut.* **2006**, *173*, 57−69.

(10) Lapka, J. L.; Paulenova, A.; Alyapyshev, M. Y.; Babain, V. A.; Herbst, R. S.; Law, J. D. *Radiochim. Acta* **2009**, *97*, 291−296.

(11) Schmitt, P.; Beer, P. D.; Drew, M. G. B.; Sheen, P. D. *Tetrahedron Lett.* **1998**, *39*, 6383−6386.

(12) Semião, A. J. C.; Rossiter, H. M. A.; Schäfer, A. I. *J. Membr. Sci.* **2010**, *348*, 174−180.

(13) Mellah, A.; Chegrouche, S.; Barkat, M. *J. Colloid Interface Sci.* **2006**, *296*, 434−441.

(14) Jang, J. H.; Dempsey, B. A.; Burgos, W. D. *Environ. Sci. Technol.* **2007**, *41*, 4305−4310.

(15) Al-Attar, L.; Dyer, A. *J. Mater. Chem.* **2002**, *12*, 1381−1386.

(16) Fryxell, G. E.; Lin, Y. H.; Fiskum, S.; Birnbaum, J. C.; Wu, H.; Kemner, K.; Kelly, S. *Environ. Sci. Technol.* **2005**, *39*, 1324−1331.

(17) Liu, W.; Zhao, X.; Wang, T.; Zhao, D. Y.; Ni, J. R. *Chem. Eng. J.* **2016**, *286*, 427−435.

(18) Kausar, A.; Bhatti, H. N. *J. Chem. Soc. Pak.* **2013**, *35*, 1041−1052.

(19) Rosenberg, E.; Pinson, G.; Tsosie, R.; Tutu, H.; Cukrowska, E. *Johnson Matthey Technol. Rev.* **2016**, *60*, 59−77.

(20) Grabias, E.; Gladysz-Plaska, A.; Ksiazek, A.; Majdan, M. *Environ. Chem. Lett.* **2014**, *12*, 297−301.

(21) Misaelides, P.; Godelitsas, A.; Filippidis, A.; Charistos, D.; Anousis, I. *Sci. Total Environ.* **1995**, *173*, 237−246.

(22) Al-Hobaib, A. S.; Al-Suhybani, A. A. *J. Radioanal. Nucl. Chem.* **2014**, *299*, 559−567.

(23) Starvin, A. M.; Rao, T. P. *Talanta* **2004**, *63*, 225−232.

(24) Ulusoy, H. I.; Simsek, S. *J. Hazard. Mater.* **2013**, *254*, 397−405.

(25) Yue, Y. F.; Mayes, R. T.; Kim, J.; Fulvio, P. F.; Sun, X. G.; Tsouris, C.; Chen, J. H.; Brown, S.; Dai, S. *Angew. Chem., Int. Ed.* **2013**, *52*, 13458−13462.

(26) Liu, M. C.; Chen, C. L.; Wen, T.; Wang, X. K. *Dalton Trans.* **2014**, *43*, 7050−7056.

(27) Carboni, M.; Abney, C. W.; Liu, S. B.; Lin, W. B. *Chem. Sci.* **2013**, *4*, 2396−2402.

(28) Wang, L. L.; Luo, F.; Dang, L. L.; Li, J. Q.; Wu, X. L.; Liu, S. J.; Luo, M. B. *J. Mater. Chem. A* **2015**, *3*, 13724−13730.

(29) Yang, W. T.; Bai, Z. Q.; Shi, W. Q.; Yuan, L. Y.; Tian, T.; Chai, Z. F.; Wang, H.; Sun, Z. M. *Chem. Commun.* **2013**, *49*, 10415−10417.

(30) McKinley, J. P.; Zachara, J. M.; Smith, S. C.; Turner, G. D. *Clays Clay Miner.* **1995**, *43*, 586−598.

(31) Manos, M. J.; Ding, N.; Kanatzidis, M. G. *Proc. Natl. Acad. Sci. U. S. A.* **2008**, *105*, 3696−3699.

(32) Manos, M. J.; Malliakas, C. D.; Kanatzidis, M. G. *Chem. - Eur. J.* **2007**, *13*, 51−58.

(33) Manos, M. J.; Iyer, R. G.; Quarez, E.; Liao, J. H.; Kanatzidis, M. G. *Angew. Chem., Int. Ed.* **2005**, *44*, 3552−3555.

(34) Mertz, J. L.; Fard, Z. H.; Malliakas, C. D.; Manos, M. J.; Kanatzidis, M. G. *Chem. Mater.* **2013**, *25*, 2116−2127.

(35) Feng, M. L.; Kong, D. N.; Xie, Z. L.; Huang, X. Y. *Angew. Chem., Int. Ed.* **2008**, *47*, 8623−8626.

(36) Ding, N.; Kanatzidis, M. G. *Nat. Chem.* **2010**, *2*, 187−191.

(37) Manos, M. J.; Kanatzidis, M. G. *Chem. Sci.* **2016**, *7*, 4804−4824.

(38) Manos, M. J.; Kanatzidis, M. G. *Chem. - Eur. J.* **2009**, *15*, 4779−4784.

DOI: 10.1021/jacs.6b07351
J. Am. Chem. Soc. 2016, 138, 12578−12585

(39) Manos, M. J.; Kanatzidis, M. G. *J. Am. Chem. Soc.* **2012**, *134*, 16441−16446.
(40) Sarma, D.; Malliakas, C. D.; Subrahmanyam, K. S.; Islam, S. M.; Kanatzidis, M. G. *Chem. Sci.* **2016**, *7*, 1121−1132.
(41) Ma, S. L.; Huang, L.; Ma, L. J.; Shim, Y.; Islam, S. M.; Wang, P. L.; Zhao, L. D.; Wang, S. C.; Sun, G. B.; Yang, X. J.; Kanatzidis, M. G. *J. Am. Chem. Soc.* **2015**, *137*, 3670−3677.
(42) Riley, B. J.; Chun, J.; Um, W.; Lepry, W. C.; Matyas, J.; Olszta, M. J.; Li, X. H.; Polychronopoulou, K.; Kanatzidis, M. G. *Environ. Sci. Technol.* **2013**, *47*, 7540−7547.
(43) Ding, N.; Kanatzidis, M. G. *Chem. Mater.* **2007**, *19*, 3867−3869.
(44) Feng, M. L.; Qi, X. H.; Zhang, B.; Huang, X. Y. *Dalton Trans.* **2014**, *43*, 8184−8187.
(45) Zhang, B.; Feng, M. L.; Cui, H. H.; Du, C. F.; Qi, X. H.; Shen, N. N.; Huang, X. Y. *Inorg. Chem.* **2015**, *54*, 8474−8481.
(46) Qi, X. H.; Du, K. Z.; Feng, M. L.; Li, J. R.; Du, C. F.; Zhang, B.; Huang, X. Y. *J. Mater. Chem. A* **2015**, *3*, 5665−5673.
(47) Li, J. R.; Huang, X. Y. *Dalton Trans.* **2011**, *40*, 4387−4390.
(48) Wang, K. Y.; Feng, M. L.; Li, J. R.; Huang, X. Y. *J. Mater. Chem. A* **2013**, *1*, 1709−1715.
(49) Venkatesan, K. A.; Shyamala, K. V.; Antony, M. P.; Srinivasan, T. G.; Rao, P. R. V. *J. Radioanal. Nucl. Chem.* **2008**, *275*, 563−570.
(50) Cheira, M. F.; El-Didamony, A. M.; Mahmoud, K. F.; Atia, B. M. *IOSR J. Appl. Chem.* **2014**, *7*, 32−40.
(51) Panturu, R. I.; Jinescu, G.; Panturu, E.; Filcenco-Olteanu, A.; Radu, D. A. *Rev. Chim.* **2011**, *62*, 814−817.
(52) Chondroudis, K.; McCarthy, T. J.; Kanatzidis, M. G. *Inorg. Chem.* **1996**, *35*, 840−844.
(53) Kanatzidis, M. G.; McCarthy, T. J.; Tanzer, T. A.; Chen, L.-H.; Iordanidis, L.; Hogan, T.; Kannewurf, C. R.; Uher, C.; Chen, B. *Chem. Mater.* **1996**, *8*, 1465−1474.
(54) Parise, J. B.; Ko, Y.; Rijssenbeek, J.; Nellis, D. M.; Tan, K.; Koch, S. *J. Chem. Soc., Chem. Commun.* **1994**, 527−527.
(55) Marking, G. A.; Kanatzidis, M. G. *Chem. Mater.* **1995**, *7*, 1915−1921.
(56) Tan, K. M.; Ko, Y. G.; Parise, J. B. *Acta Crystallogr., Sect. C: Cryst. Struct. Commun.* **1995**, *51*, 398−401.
(57) Jiang, T.; Lough, A.; Ozin, G. A. *Adv. Mater.* **1998**, *10*, 42−46.
(58) Bowes, C. L.; Petrov, S.; Vovk, G.; Young, D.; Ozin, G. A.; Bedard, R. L. *J. Mater. Chem.* **1998**, *8*, 711−720.
(59) Jiang, T.; Lough, A.; Ozin, G. A.; Bedard, R. L.; Broach, R. *J. Mater. Chem.* **1998**, *8*, 721−732.
(60) Zhao, Y. G.; Li, J. X.; Zhang, S. W.; Chen, H.; Shao, D. D. *RSC Adv.* **2013**, *3*, 18952−18959.
(61) Zhang, L.; Zhang, L.; Wu, T. H.; Jing, X. Y.; Li, R. M.; Liu, J. Y.; Liu, Q.; Wang, J. *RSC Adv.* **2015**, *5*, 53433−53440.
(62) Yin, Z. L.; Xiong, J.; Chen, M.; Hu, S.; Cheng, H. M. *J. Radioanal. Nucl. Chem.* **2016**, *307*, 1471−1479.
(63) Lehto, J.; Clearfield, A. *J. Radioanal. Nucl. Chem.* **1987**, *118*, 1−13.
(64) Do, D. D. *Adsorption Analysis: Equilibria and Kinetics*; Imperial College Press: London, 1998.
(65) Abdel-Ghani, N. T.; Rawash, E. S. A.; El-Chaghaby, G. A. *Global J. Environ. Sci. Manage.* **2016**, *2*, 11−18.
(66) Li, J.; Chen, Z.; Wang, R. J.; Proserpio, D. M. *Coord. Chem. Rev.* **1999**, *192*, 707−735.
(67) Feng, M.-L.; Wang, K.-Y.; Huang, X.-Y. *Chem. Rec.* **2016**, *16*, 582−600.

DOI: 10.1021/jacs.6b07351
J. Am. Chem. Soc. 2016, 138, 12578−12585